Theoretical and Applied Genetics (2025) 138:107
https://doi.org/10.1007/s00122-025-04900-4

ORIGINAL ARTICLE

Joint linkage and association analysis identifies genomic regions and candidate genes for yield-related traits in wheat

Lei Zhuang[1] · Lifeng Du[2] · Haixia Liu[1] · Hongxia Liu[1] · Huifang Li[3] · Yinhui Zhang[1] · Yunchuan Liu[1] · Jian Hou[1] · Tian Li[1] · Delong Yang[4] · Xueyong Zhang[1] · Chenyang Hao[1]

Received: 21 December 2024 / Accepted: 4 April 2025 / Published online: 2 May 2025

Abstract

Key message **Twenty-six QTLs associated with yield-related traits in wheat were identified through joint linkage and association analysis, with *TraesCS5A03G0002500* being selected as a candidate gene for *QGl.caas-5A.1*.**

Abstract As a major staple crop worldwide, continuously increasing wheat yield is crucial for ensuring food security. Wheat yield is influenced by multiple traits, and elucidating the genetic basis of yield-related traits lays a foundation for future gene cloning and molecular mechanism studies. In this study, a recombinant inbred line (RIL) population derived from 292 lines of Hengguan 35/Zhoumai 18 was genotyped with the Affymetrix wheat 660 K SNP array. Combined with the phenotype of the RIL population in 13 environments, linkage analysis of six yield-related traits including plant height, grain number per spike, thousand-grain weight, grain length, grain width, and grain thickness was conducted. A total of 262 quantitative trait locus (QTLs) (logarithm of odds [LOD] > 3) were identified across 21 chromosomes, in which 50 QTLs were repeatedly detected in more than three environments. Numerous QTLs harbored cloned genes and overlapped with those reported in previous studies. Subsequently, joint analysis of genome-wide association study (GWAS) data from the advanced backcross-nested association mapping plus inter-crossed (AB-NAMIC) population and QTLs identified in the RIL population revealed 26 overlapping genomic regions. Notably, the *QGl.caas-5A.1* associated with grain length on chromosome 5A was detected in both the RIL and AB-NAMIC populations, and *TraesCS5A03G0002500* was selected as a candidate gene. A kompetitive allele-specific PCR (KASP) marker based on a variant [A/G] in *TraesCS5A03G0002500* was developed and validated in a natural population containing 350 accessions. Taken together, these results provide valuable information for fine mapping and cloning of yield-related wheat genes in the future.

Keywords Wheat · Yield-related traits · 660 K SNP array · QTL mapping · KASP

Introduction

Common wheat (*Triticum aestivum* L.) is an important staple crop that feeds approximately 40% of the world's population (Xiao et al. 2022). China is the largest wheat producer

Communicated by Jiankang Wang.

Lei Zhuang, Lifeng Du and Haixia Liu have contributed equally to this work.

✉ Delong Yang
yangdl@gsau.edu.cn

✉ Xueyong Zhang
zhangxueyong@caas.cn

✉ Chenyang Hao
haochenyang@caas.cn

[1] State Key Laboratory of Crop Gene Resources and Breeding/ National Key Facility for Crop Gene Resources and Genetic Improvement, Institute of Crop Sciences, Chinese Academy of Agricultural Sciences, Beijing 100081, China

[2] Jiaozuo Academy of Agricultural and Forestry Sciences, Jiaozuo 454000, Henan, China

[3] State Key Laboratory of Wheat and Maize Crop Science, and Center for Crop Genome Engineering, College of Agronomy, Henan Agricultural University, Zhengzhou 450046, China

[4] State Key Laboratory of Aridland Crop Science, Gansu Agricultural University, Lanzhou 730070, China

and consumer in the world (Gupta et al. 2020). Given the increasing world population and decreasing cultivated land area, increasing wheat yield per unit area is an important goal of current breeding programs. Grain yield is a comprehensive trait that is affected by multiple factors. Generally, thousand-grain weight, grain number per spike, and spike number per unit area are usually defined as the three components of wheat yield. In addition, important agronomic traits, such as heading date and plant height, have different degrees of correlation with the three wheat yield components, indirectly affecting wheat yield (Simmonds et al. 2014; Lopes et al. 2012). Yield-related traits are quantitative traits influenced by multiple genes with minor effects and are susceptible to environmental factors. Linkage analysis and association mapping based on forward genetics are two effective approaches for discovering quantitative trait locus (QTL) (Cadic et al. 2013; Khan et al. 2021).

Numerous QTLs and genes associated with grain yield have been identified in wheat. Specifically, 25 genes influencing plant height have been identified (McIntosh et al. 2020). These genes play pivotal roles in modulating the plant architecture of wheat, which in turn affects grain yield by influencing factors such as lodging resistance and the harvest index (Gale and Youssefian 1985). Notably, *RHB-B1*, *RHT-D1*, and *RHT8* have been successfully cloned and are the most widely utilized wheat dwarfing genes worldwide (Chai et al. 2022). Efforts to improve grain yield have been constrained by the trade-off between grain weight/size and grain number (Quintero et al. 2018). The number of grains per spike depends on floret fertility and the number of spikelets per spike. Many flowering time-related genes (*FT1*, *Ppd-1*, *VRN1*, and *FUL2*) affect spikelet and grain numbers per spike by regulating early spike development (Finnegan et al. 2018). Additionally, *GNI1* (Sakuma et al. 2019), *TaSUT1* (Al-Sheikh Ahmed et al. 2018), *TaPIN1* (Wang et al. 2017a, b), and *TaSPL14* (Cao et al. 2021), among others, regulate the number of grains per spike in wheat. Many genes controlling grain size have been cloned in rice, such as those involved in the ubiquitin–proteasome pathway like *GW2* (Song et al. 2007), *WTG1* (Huang et al. 2017), and *OsOTUB1* (Wang et al. 2017a, b); G-protein signaling such as *GS3* (Sun et al. 2018) and *DEP1* (Huang et al. 2009); and phytohormone signaling and homeostasis including *GS5* (Li et al. 2011), *GSK2* (Tong et al. 2012), and *GL3.1* (Qi et al. 2012). Recently, numerous genes related to grain weight/size in wheat, e.g., *TaGW2* (Hong et al. 2014), *TaDEP1* (Li et al. 2022), and *Tasg-D1* (Cheng et al. 2020), have been cloned via reverse genetics strategies. However, few yield-related genes have been cloned through forward genetics, and further research is needed.

Currently, a series of single-nucleotide polymorphism (SNP) arrays have been designed for genomic research and molecular breeding using marker-assisted selection (MAS) in various crop species. For wheat, 9 K and 90 K chips based on Illumina Infinium BeadChip technology, as well as 660 K, 820 K, and 35 K arrays based on Affymetrix Axiom technology, have been successively developed (Rasheed et al. 2017). The 660 K array contains 630,517 SNP loci, with approximately 75.8% of the markers located in intergenic regions and 24.2% in genic regions. This array addresses the disadvantage of limited markers in the D subgenome and has a relatively uniform distribution of markers across the genome. The 660 K array has tremendous potential in the genotyping and molecular marker selection of polyploid wheat (Sun et al. 2020) and has been widely applied in various genetic studies, including comparative genomics (Zhou et al. 2018), linkage map construction and QTL mapping (Cui et al. 2017), and genome-wide association analysis (Yang et al. 2019; Niaz et al. 2023).

Wheat is an allopolyploid with a genome size of ~ 16 Gb and 80% DNA repeats (Xiao et al. 2022). The number of genes cloned from wheat is much lower than those cloned from rice, maize, and other crops. A large number of studies have preliminarily dissected the genetic basis of wheat yield-related traits via linkage analysis or genome-wide association studies (GWAS) and identified numerous QTLs. However, linkage analysis typically requires the construction of a specific genetic population, a process that is time-consuming and constrained by parental mating types. Limited recombination events result in broad mapping intervals, making it difficult to fine-map target genes (Liang et al. 2021). On the other hand, GWAS, although conducted in natural populations, is susceptible to population stratification, which may lead to false positive results if not properly controlled, particularly in the detection of low-frequency and rare variants, where the effectiveness of this method is weaker (OTT et al. 2015; Sazonovs and Barrett 2018). Therefore, a joint linkage analysis with a GWAS, important genomic regions, and critical genes associated with yield-related traits can be rapidly discovered (Bergelson and Roux 2010), laying the foundation for subsequent gene cloning and elucidation of the underlying molecular mechanism.

In our previous studies, a GWAS was performed on 11 yield-related traits using an advanced backcross-nested association mapping plus inter-crossed (AB-NAMIC) population comprising 590 lines. Specifically, the AB-NAMIC population was enriched in beneficial traits, and a large number of substantial GWAS signals were detected (Jiao et al. 2023). In the present study, the wheat 660 K array was used to genotype the recombinant inbred line (RIL) population derived from Hengguan 35/Zhoumai 18, and linkage analysis of yield-related traits was carried out in combination with phenotypic data. The candidate regions for yield-related traits were mapped through comparative analysis of the RIL and AB-NAMIC populations. The

objectives of this study were to: (1) construct a high-density genetic map suitable for QTL mapping based on the Affymetrix wheat 660 K SNP array, (2) integrate linkage analysis with GWAS to perform a joint analysis of yield-related traits and identify important genomic regions, (3) predict candidate gene for targeted QTL interval according to reference genome annotation information and expression patterns, and (4) develop practicable kompetitive allele-specific PCR (KASP) marker of the candidate gene and verify the marker in a natural population consisted of 350 accessions for MAS in high-grain length wheat breeding. Overall, this study aimed to provide valuable information for wheat yield molecular breeding by co-anchoring yield-related genomic regions in different genetic populations.

Materials and methods

Plant materials

A mapping population composed of 292 RILs derived from Hengguan 35/Zhoumai 18 was used as the study material. The RIL population was constructed by the single-seed descent method, and a stable F_{14} family was formed via continuous self-crossing from F_2. Hengguan 35 is a winter wheat cultivar bred from Heng84-Guan749 and Heng87-4263 in Hebei, China; this cultivar has short stalks, large spikes, early maturity, high yield, water savings, and multiresistance. Zhoumai 18, developed by crossing Neixiang 185 with Zhoumai 9 in Henan, China, exhibits characteristics such as a high tillering-to-panicle ratio, medium maturity, high stable yield potential, and wide adaptability. The RIL population generally exhibited moderate resistance to powdery mildew and stripe rust under field conditions. In addition, a natural population of 350 accessions, comprising 113 Chinese landraces, 226 modern Chinese cultivars, and 11 introduced cultivars (Table S1), was used for KASP marker screening.

Field trials and phenotypic evaluation

Field experiments were conducted at the Zhengzhou Experimental Station, Henan (113.7°E, 34.8°N), in 2014; Chinese Academy of Agricultural Sciences (CAAS)-Xinxiang Experimental Station, Henan (113.5°E, 35.2°N), from 2015–2020; and CAAS-Shunyi Experimental Station, Beijing (116.3°E, 40.0°N), from 2015–2020. Both parents and the 292 RILs were planted in those 13 environments. In addition, a natural population consisting of 350 accessions was planted at Xinxiang Experimental Station from 2016 to 2019. Hereafter, the 13 phenotypic identification environments were designated 2014-Zhengzhou, 2015-Xinxiang, 2015-Shunyi, 2016-Xinxiang, 2016-Shunyi, 2017-Xinxiang, 2017-Shunyi, 2018-Xinxiang, 2018-Shunyi, 2019-Xinxiang, 2019-Shunyi, 2020-Xinxiang, and 2020-Shunyi, respectively. Field experiments were grown in a randomized block design with three replications. Each accession was planted in a 2-m four-row plot with 25 cm between rows and 20 seeds per row. Field management followed local practices. The six agronomic traits were investigated in the RIL population according to the Descriptors and Data Standard for wheat (Li and Li 2006), including plant height (PH, cm), grain number per spike (GN), thousand-grain weight (TGW, g), grain length (GL, mm), grain width (GW, mm), and grain thickness (GT, mm). In the natural population, four traits, namely TGW, GL, GW, and GT, were measured. Specifically, at physiological maturity, ten plants from the middle rows in each plot were selected to determine PH and GN. PH was measured as the length from the soil surface to the top of the spike (excluding awns); GN was the total number of grains per spike. After physiological maturity, spikes in the middle two rows were hand-harvested to determine TGW, GL, GW, and GT. Harvested wheat grains were air-dried to a 12% water content and then weighed. Grain-related traits were measured semiautomatically by an SC-G automatic grain analyzer (Hangzhou Wanshen Testing Technology Co., Ltd.).

Phenotypic statistical analysis

The best linear unbiased prediction (BLUP) values for each trait from different environments were calculated using the "lme4" package in R (Bates et al. 2015). The formula of model for BLUP was as follows: $Y=\mu+\text{Line}+\text{Loc}+(\text{Line}\times\text{Loc})+\text{Rep (Loc)}+\varepsilon$, where Y represents the phenotype; μ represents the intercept; Line and Loc denote the respective random effects of the genotype and the environment; Line × Loc is the interaction effect between genotype and environment; Rep (Loc) is the random effect of replication nested in the environment; and ε represents the random residual error effect. Basic descriptive statistics and analysis of variance (ANOVA) were conducted using SPSS v25.0 (https://www.ibm.com/spss). The formula ($H^2=\sigma_g^2/(\sigma_g^2+\frac{\sigma_{ge}^2}{n}+\frac{\sigma_e^2}{nr})$) was used to calculate the broad-sense heritability (H^2), where σ_g^2, σ_{ge}^2 and σ_e^2 represent the variance components of genotype, interaction between genotype and environment, and error, respectively, r is the number of replicates, and n denotes the number of environments for phenotypic assessment. Pearson's correlations between traits were calculated using the BLUP values with the "PerformanceAnalytics" package in R (https://github.com/braverock/PerformanceAnalytics). The analysis of normal distribution was conducted with Origin software (https://www.originlab.com/). Additionally, visualization was

performed with the "ggplot2" package in R (Villanueva and Chen 2019).

Genotyping and construction of the genetic map

All the lines and both parents of the RIL population were planted in the greenhouse of the Institute of Crop Sciences, Chinese Academy of Agricultural Sciences (116.3°E, 40.0°N). When the seedlings reached the three-leaf stage, partial leaf samples were collected for whole-genome DNA extraction. The wheat genomic DNA was extracted using a fast plant genomic DNA extraction kit (Tiangen Biochemical Technology Co., Ltd., DP321) according to the manufacturer's instructions. After preliminary testing for DNA quality and purity using a 1% agarose gel, the qualified samples were sent to Beijing CapitalBio Technology Co., Ltd. (http://www.capitalbiotech.com/), and the Affymetrix wheat 660 K SNP array was used to genotype 294 samples. On the basis of the genotyping results, three categories of poor-quality genotypes were removed: mono high resolution (clear clustering, but lacking one homozygous marker), call rate below threshold (low response, poor genotyping), and other (poor genotyping and unmapped to chromosomes). Furthermore, the genotype data of Hengguan 35 and Zhoumai 18 were compared, and SNP markers with homozygous genotypes and with different allelic variations ("aa × bb" type) between the parents were extracted. The genotypes of the RIL population were extracted for the polymorphic SNP markers identified between the parents, and the heterozygous markers in the progeny were converted to missing types. Then, SNP marker quality control was performed using the VCFtools software (Danecek et al. 2011) with parameter thresholds set as follows: minor allele frequency (MAF) ≥ 0.05 and missing rate ≤ 0.1.

A redundancy analysis of high-quality polymorphic SNP loci based on the separation pattern of the RIL population was conducted using the BIN module of IciMapping 4.2 software (Meng et al. 2015). The "missing rate" and "*P* value for segregation distortion test" parameters were set to 10% and 0.001, respectively. One marker was randomly selected from each bin for genetic map construction. The bin markers were grouped according to the chromosome information from the Affymetrix wheat 660 K SNP array, and a genetic map was constructed using the maximum likelihood (ML) method in JoinMap 4.0 software (Stam 1993). The conversion between the recombination rate and genetic distance was performed via the Kosambi function. The genetic map was plotted using the "LinkageMapView" package in R (Ouellette et al. 2017) and MapChart (Voorrips 2002. https://doi.org/https://doi.org/10.1093/jhered/93.1.77). The quality of the genetic map was assessed by collinearity analysis between the genetic map and the physical map. The correlation coefficients between the genetic positions and the physical positions of the markers were calculated by Excel. The collinearity between the genetic and physical maps was visualized using the "Circlize" package in R (Gu et al. 2014).

QTL mapping

QTL mapping for yield-related traits was performed using the inclusive composite interval mapping (ICIM) method in the BIP module of IciMapping 4.2 software (Li et al. 2008; Meng et al. 2015). The parameters were set as follows: step size = 0.1 cM, probability in stepwise regression (PIN) = 0.001, and threshold of logarithm of odds (LOD) value ≥ 3. The QTLs associated with the same trait, located within a genetic distance of approximately 10 cM on the same chromosome, were merged and considered as a single QTL. Additionally, QTLs detected in more than three environments were considered stable major QTLs. The QTL was named following the method proposed by Liu et al. (2018a, b), which was formatted as "Q + trait abbreviation + research facilities abbreviation + chromosome name + order on the chromosome." In addition, according to breeding selection objectives and previous studies (Pang et al. 2020), the variations that increased GN, TGW, GL, GW, and GT, while moderately decreased PH were defined as favorable alleles in this study. QTL cluster analysis was then performed on stable QTLs associated with six yield-related traits. When two or more stable QTLs were located within a specific chromosomal region (≤ 20 cM), they were grouped into a single QTL cluster.

Overlapping genomic regions between the RIL and AB-NAMIC populations

The flanking sequences of the QTLs identified by linkage mapping were aligned to the Chinese Spring reference genome (IWGSC RefSeq v2.1) to determine their physical position. Based on the GWAS signals from our previous study of Jiao et al. (2023), the merge command of Bedtools was used to merge overlapping QTLs identified for each trait into a new QTL. The QTLs identified by linkage analysis in the RIL population were subsequently compared with those detected via GWAS in the AB-NAMIC population, and the overlapping QTLs between the two populations were obtained when the physical positions of their intervals partially overlapped with a minimum distance of ≥ 0.5 Mb.

Candidate gene prediction and KASP marker development

The IntervalTool tool on the WheatOmics 1.0 website (http://wheatomics.sdau.edu.cn/) was utilized to obtain candidate genes within high-confidence genomic regions. The expression patterns of the candidate genes were

analyzed using the Wheat Expression Browser database (http://www.wheat-expression.com/). The SNP tightly linked to the *QGl.caas-5A.1*, and the variant of [A/G] on the second intron of the candidate gene was converted into a KASP marker (Table S2). The natural population was genotyped using the developed KASP markers to preliminarily validate gene function. KASP reactions were carried out on QuantStudio™ 7 Flex (Applied Biosystems by Life Technologies, San Diego, CA, USA) using the KASP V4.0 2×Master mix (LGC Genomics, Teddington, UK) as previously described (Zhao et al. 2019).

Results

Phenotypic variation and correlation analysis

The basic descriptive statistics for PH, GN, TGW, GL, GW, and GT indicated significant phenotypic differences in GN and GT between the parents, whereas the differences in other traits were not significant (Fig. 1, Table 1). Compared with Hengguan 35, Zhoumai 18 had a greater GT but a smaller GN. However, the range

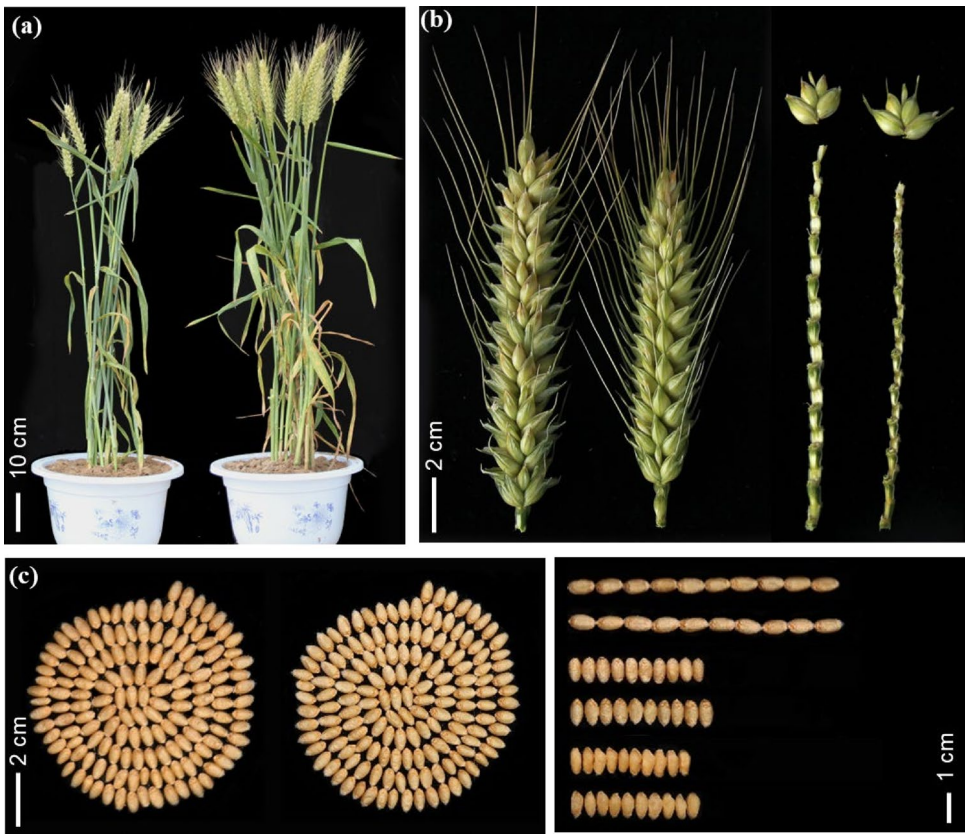

Fig. 1 Phenotypic characterization of Hengguan 35 and Zhoumai 18. **a** Morphology of the whole plants of the parental lines Hengguan 35 and Zhoumai 18. **b** Spike morphology of the parental lines Hengguan 35 and Zhoumai 18. **c** Grain size of the parental lines Hengguan 35 and Zhoumai 18. The left figure shows the 150-grain sizes of Hengguan 35 and Zhoumai 18, and the figure on the right shows the grain length, width, and thickness of Hengguan 35 and Zhoumai 18, respectively

Table 1 Basic descriptive statistics of the RIL parents and lines based on BLUP values

Trait[a]	Parents		RIL lines					
	Hengguan 35	Zhoumai 18	Mean ± S.E.[b]	Range	*CV* (%)[c]	Kurtosis	Skewness	H^2 (%)[d]
PH	69.82	68.41	73.82 ± 1.00	37.88–116.58	23.19	-0.33	0.32	98.95
GN	57.97	53.84 *	52.58 ± 0.31	39.87–64.82	10.12	-0.72	0.11	84.46
TGW	45.75	49.29	48.22 ± 0.26	35.07–58.17	9.17	-0.30	-0.38	89.73
GL	6.58	6.62	6.55 ± 0.01	6.12–7.12	2.76	0.20	0.44	90.06
GW	3.44	3.57	3.52 ± 0.01	3.11–3.83	3.72	-0.29	-0.32	88.55
GT	3.01	3.17 *	3.11 ± 0.01	2.82–3.36	3.65	-0.65	-0.07	83.83

[a]PH, plant height (cm); GN, grain number per spike (number); TGW, thousand-grain weight (g); GL, grain length (mm); GW, grain width (mm); GT, grain thickness (mm). [b]S.E., standard error; [c]*CV*, coefficient of variation; [d]H^2, broad-sense heritability. *indicates significant differences at $P < 0.05$

of coefficient of variation (*CV*) of the six yield-related traits in the RIL population was quite wide, ranging from 2.76% to 23.19%. The BLUP values exhibited a continuous distribution, ranging from 37.88 cm to 116.58 cm for PH, 39.87 to 64.82 for GN, 35.07 g to 58.17 g for TGW, 6.12 mm to 7.12 mm for GL, 3.11 mm to 3.83 mm for GW, and 2.82 mm to 3.36 mm for GT. The broad-sense heritability (H^2) was high, greater than 80%, for all six traits, indicating that these traits were less affected by the environment and could be inherited stably in the RIL population.

Correlation analysis showed that in the RIL population, PH had a significant negative correlation with GN, whereas there was a significant positive correlation between PH and grain weight-related traits, *i.e.,* TGW, GL, GW, and GT. There was a significant negative correlation between GN and grain weight-related traits, and TGW had a significant positive correlation with GL, GW, and GT (Fig. 2a). Additionally, all traits exhibited a continuous distribution in the RIL population, with absolute skewness and kurtosis values of less than 1.0 for all the traits, indicating that these traits largely conformed to a normal distribution (Fig. 2b, Table 1).

Bin-based genetic map construction and assessment

The Affymetrix wheat 660 K SNP array was used to genotype 292 RILs. On the basis of the SNP marker flanking sequence alignment to the Chinese Spring reference genome (IWGSC RefSeq v2.1), the specific physical positions of 66,063 (10.48%) high-quality polymorphic SNP markers between the parents were obtained (Table S3). Figure 3a shows the distribution of those SNP markers on the physical map across 21 wheat chromosomes. Generally, the segregation ratio of the two alleles for one SNP marker in the RIL population is 1:1. In this study, after removing SNPs with $P < 0.001$ via a partial segregation test, the remaining 51,536 (8.17%) SNP markers were used for genetic map construction, and these markers were divided into 2,890 bins. A genetic map containing 21 wheat chromosomes with a length of 4,243.31 cM was successfully constructed (Fig. 3b). More precisely, the lengths of the A, B, and D subgenomes were 1,494.81 cM, 1422.33 cM, and 1,326.17 cM, respectively. The genetic length of different chromosomes ranged from 80.20 cM (1B) to 277.41 cM (5B), with an average of 202.06 cM. The collinearity analysis of the genetic map and the physical map revealed that the SNP order in the genetic map had good collinearity with that in the assembly of the wheat reference genome (Fig. 3c), indicating that the genetic map constructed in this study was of high quality.

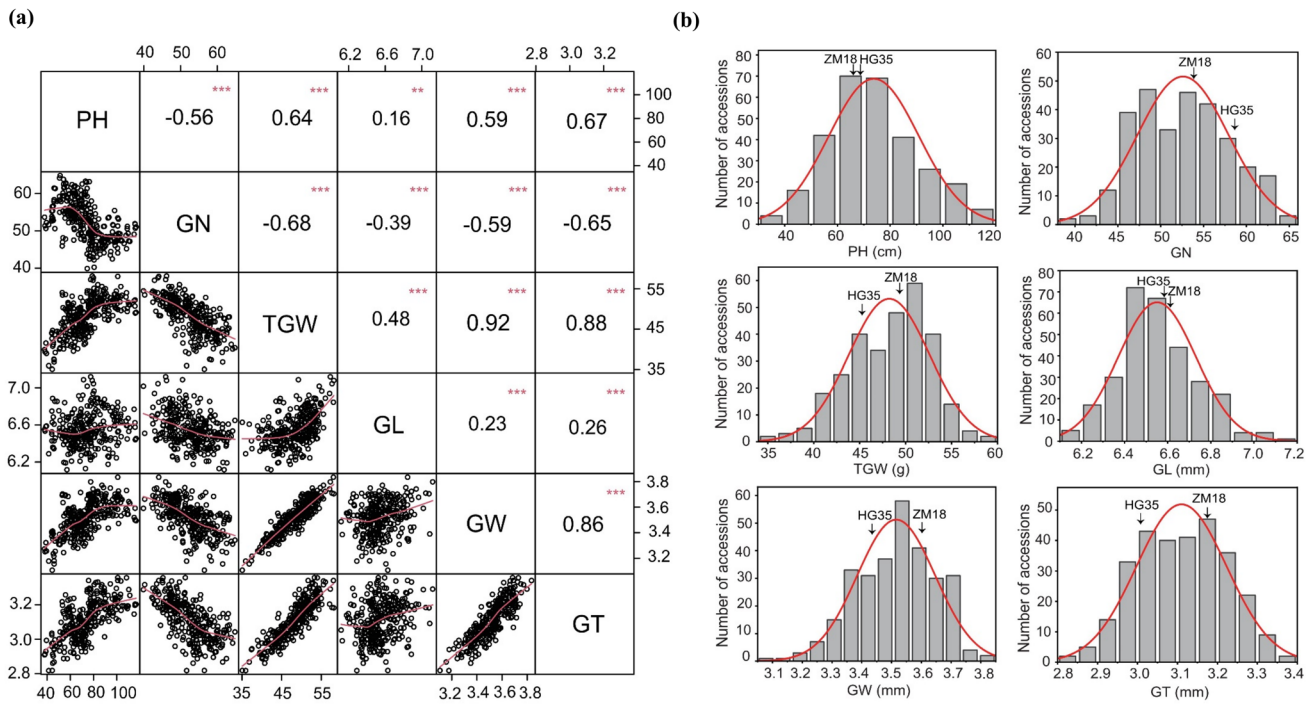

Fig. 2 Pearson correlation and normal distribution analysis of six yield-related traits in the RIL populations based on the BLUP values. **a** Pearson correlation analysis of yield-related traits. **, *** represent significance at $P < 0.01$ and $P < 0.001$, respectively. **b** Normal distribution analysis of traits in the RIL population

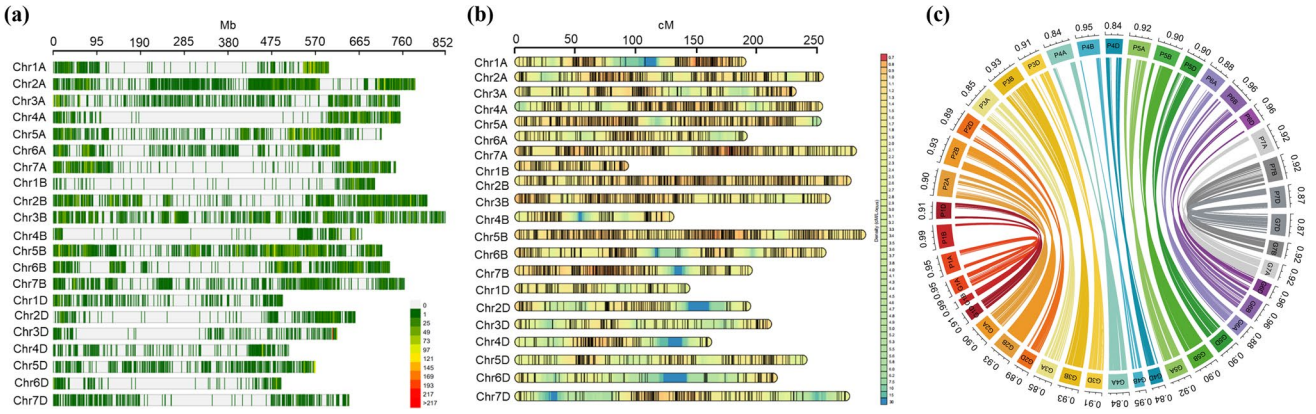

Fig. 3 Bin-based genetic map construction and quality assessment. **a** Distribution of 66,063 high-quality polymorphic SNP markers on the physical map across 21 chromosomes. **b** Genetic map of 21 chromosomes in the RIL population. **c** Collinearity analysis between the genetic map and the physical map

QTL detection for yield-related traits

A total of 262 putative QTLs were detected for PH, GN, TGW, GL, GW, and GT distributed across 21 chromosomes (Table S4). Among them, 50 QTLs could be repeatedly detected in more than three environments; thus, these QTLs were considered environmentally stable (Fig. 4, Table 2). The greatest number of QTLs controlling yield-related traits was detected on chromosomes 7A and 4A, whereas only two QTLs were identified on chromosome 1D.

A total of 57 QTLs for PH were identified, 16 of which were stable QTLs detected in at least three environments (Table 2, Fig. S1). The percentage of phenotypic variance explained (PVE) ranged from 1.56% to 40.10%, with LOD values ranging from 3.36 to 46.09 for the 16 stable QTLs. Among the alleles for decreased PH, 11 QTLs were contributed by Hengguan 35 and five were contributed by Zhoumai 18. The PVEs of *QPh.caas-6A.1* (5.76%) and *QPh.caas-4D.1* (40.10%) both exceeded 5%, and these QTLs were detected in 12 environments and 13 environments, respectively.

A total of 50 QTLs for GN were identified, seven of which were stable QTLs detected in at least three environments (Table 2, Fig. S2). The PVE ranged from 2.88% to 21.90%, with LOD values ranging from 4.64 to 25.29 for the seven stable QTLs. Among the alleles for increased GN, five QTLs were contributed by Hengguan 35 and two were contributed by Zhoumai 18. The PVEs of *QGn.caas-4A.4* (5.18%) and *QGn.caas-4D.1* (21.90%) both exceeded 5%, and these QTLs detected in three environments and 13 environments, respectively.

A total of 34 QTLs for TGW were identified, seven of which were stable QTLs detected in at least three environments (Table 2, Fig. S3). The PVE ranged from 4.28% to 27.65%, with LOD values ranging from 4.77 to 28.00 for the seven stable QTLs. Among the alleles for increased TGW, three QTLs were contributed by Hengguan 35 and four were contributed by Zhoumai 18. The PVEs of *QTgw.caas-4A.5* (6.03%), *QTgw.caas-4A.6* (7.09%), and *QTgw.caas-4D.1* (27.65%) both exceeded 5%, and these QTLs were detected in five, five, and 13 environments, respectively.

A total of 58, 27, and 36 QTLs for GL, GW, and GT, respectively, were identified, of which 13, four, and three, respectively, were stable QTLs detected in at least three environments (Table 2, Figs. S4, S5 and S6). The PVE of GL ranged from 3.37% to 7.27%, with LOD values ranging from 3.85 to 13.32 for the 13 stable QTLs. The PVE of GW ranged from 2.96% to 22.55%, with LOD values ranging from 3.87 to 21.90 for the four stable QTLs. The PVE of GT ranged from 3.34% to 22.76%, with LOD values ranging from 4.05 to 21.84 for the three stable QTLs. GL, GW, and GT had six, two, and one stable QTL, respectively, with PVE values exceeding 5%.

Ten pleiotropic QTL clusters, comprising 27 stable QTLs, were identified across chromosomes 3B, 4A, 4D, 5B, 5D, and 7A (Table S5), with each cluster containing two to six QTLs. Among these, the cluster *QGt.caas-4D.1/QGl.caas-4D.1/QGn.caas-4D.1/QGw.caas-4D.1/QTgw.caas-4D.1/QPh.caas-4D.1* on chromosome 4D (spanning 51.3 cM to 62.7 cM) contained the most QTLs and exhibited positive additive effects for TGW, GL, GW, GT, and PH, while showing a negative additive effect for GN. The cluster *QPh.caas-4A.3/QGw.caas-4A.3/QGl.caas-4A.1/QTgw.caas-4A.5* on chromosome 4A (spanning 138.3 cM to149.2 cM) had a positive additive effect for PH, but negative additive effects for TGW, GL and GW. The cluster *QTgw.caas-7A.3/QGn.caas-7A.2/QGl.caas-7A.4* on chromosome 7A (spanning 165.7 cM

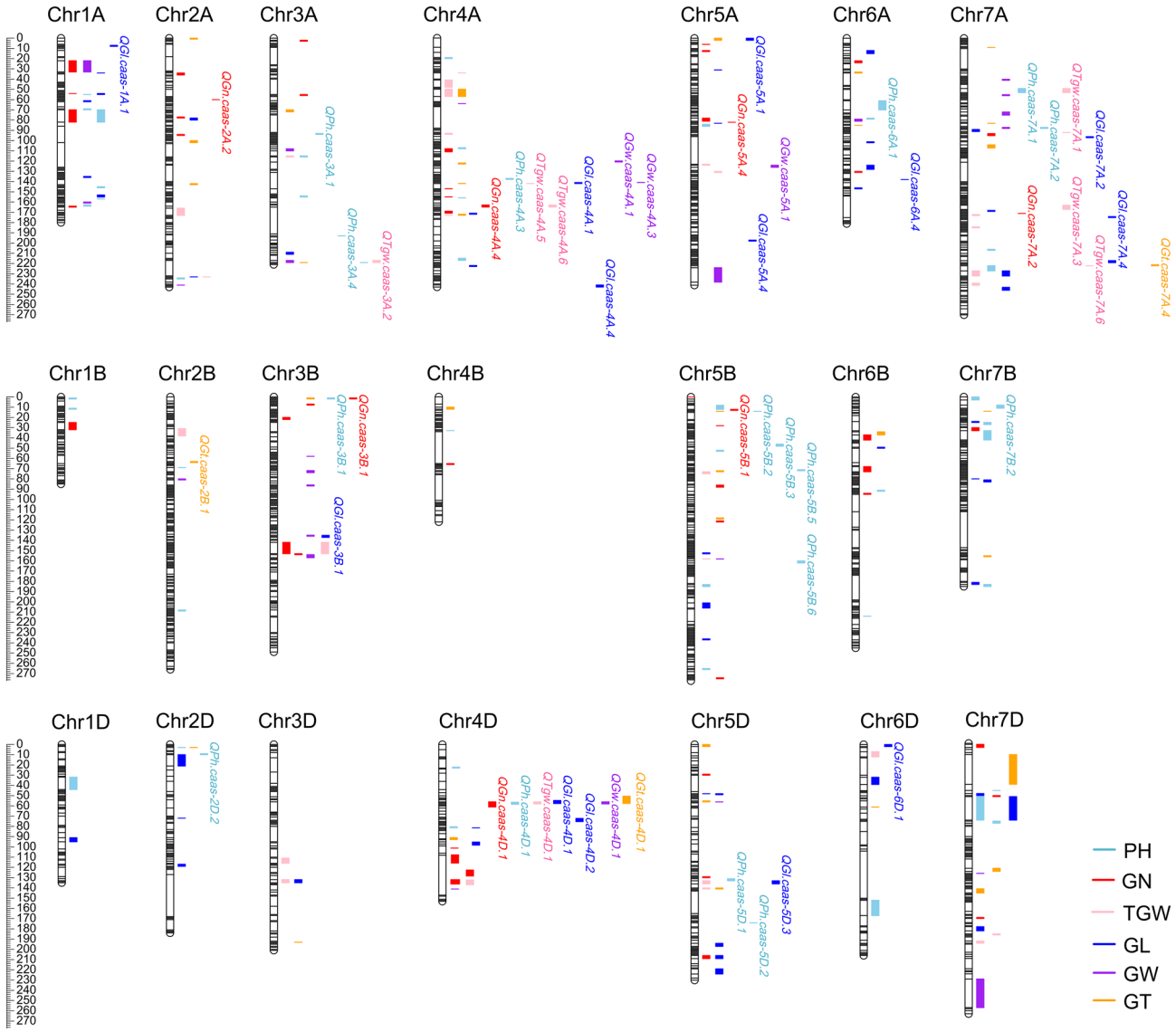

Fig. 4 Genetic position of QTL regions associated with plant height (PH), grain number per spike (GN), thousand-grain weight (TGW), grain length (GL), grain width (GW), and grain thickness (GT). Named QTLs represent stable QTLs identified in three or more environments

to 179.5 cM) exhibited a positive additive effect for TGW and a negative additive effect for GN.

Additive effect of identified QTLs in the RIL population

PH in the RIL population exhibited significant and extensive phenotypic variation, ranging from 37.9 cm to 116.6 cm, with a high *CV* of 23.2% (Fig. 5a, Table 1). Sixteen stable QTLs controlling PH were identified through linkage analysis in the RIL population, with 11 QTLs containing the allele for reduced PH from Hengguan 35 and the other five containing the allele from Zhoumai 18 (Figs. S1 and 5b). The phenotypic effect was evaluated by the linear regression between the number of reduced PH alleles and PH. The results showed that as the number of reduced PH alleles increased, PH obviously trended to decrease, and a strong negative correlation ($r^2 = 0.40$) was found, indicating that the accumulation of more alleles for reduced PH led to lower PH (Fig. 5c and d). Hence, when the RILs carried only one allele for reduced PH, the PH was 115.9 cm, whereas RILs with 13 alleles for reduced PH had the lowest average PH (55.9 cm). Similarly, there were strong positive correlations between the number of alleles for increased GN, GW, TGW, GT, and GL and the corresponding phenotypic values (Fig. S7). These results imply the reliability of QTL mapping and the significant additive effect of alleles for yield-related traits.

Table 2 Stable quantitative trait locus (QTL) for six traits identified across multiple environments in the RIL population

Trait[a]	QTL	Environment[b]	Marker interval (cM)	Left marker of peak	Right marker of peak	LOD[c]	PVE (%)[d]	Add[e]	Donor of favorable alleles	Previous reference reports[f]
PH	*QPh.caas-3A.1*	E2/E3/E10/E12/E14	94.1–96.9	*AX-108732873*	*AX-110378636*	7.33	2.98	-2.69	Hengguan 35	Zhang et al. (2017)
	QPh.caas-3A.4	E5/E7/E9/E11/E13	193.1–200.1	*AX-109343446*	*AX-111463342*	5.92	2.18	-2.96	Hengguan 35	Guan et al. (2018)
	QPh.caas-4A.3	E3/E5/E7/E6/E9/E10/E11/E12/E14	138.3–149.2	*AX-109580567*	*AX-94978517*	5.56	2.18	2.58	Zhoumai 18	Li et al. (2015)
	QPh.caas-6A.1	E2/E3/E4/E5/E6/E8/E9/E10/E11/E12/E13/E14	62.6–70.4	*AX-110975340*	*AX-109974361*	12.89	5.76	-4.22	Hengguan 35	Zhai et al. (2016)
	QPh.caas-7A.1	E5/E9/E11/E13/E14	52.8–63.9	*AX-111761655*	*AX-110395009*	7.04	2.49	-3.22	Hengguan 35	NA
	QPh.caas-7A.2	E2/E5/E8/E9/E10/E11/E12/E13/E14	88.2–91.9	*AX-111156184*	*AX-109848559*	11.03	4.10	3.80	Zhoumai 18	Hu et al. (2020)
	QPh.caas-3B.1	E3/E6/E8	1.0–2.2	*AX-110468825*	*AX-110735793*	5.62	2.63	-2.55	Hengguan 35	Cui et al. (2022)
	QPh.caas-5B.2	E2/E5/E6/E7/E9/E10/E12/E13	14.0–14.9	*AX-108871901*	*AX-109866963*	12.45	4.89	-3.94	Hengguan 35	NA
	QPh.caas-5B.3	E4/E8/E12/E14	46.9–48.0	*AX-109913757*	*AX-109845322*	6.09	2.48	-2.69	Hengguan 35	NA
	QPh.caas-5B.5	E5/E7/E9/E13/	72.2–72.4	*AX-111656355*	*AX-109492223*	7.58	2.78	-3.21	Hengguan 35	NA
	QPh.caas-5B.6	E4/E6/E8	160.6–160.8	*AX-111001298*	*AX-89376056*	3.36	1.56	-2.01	Hengguan 35	NA
	QPh.caas-7B.2	E3/E4/E6/E7/E8/E9/E10/E11/E12/E14	10.5–18.7	*AX-94780393*	*AX-109486292*	8.56	3.69	3.15	Zhoumai 18	Yan et al. (2006)
	QPh.caas-2D.2	E2/E3/E4/E6/E7/E8/E9/E10/E14	9.2–12.0	*AX-111021196*	*AX-111618622*	6.45	3.21	2.85	Zhoumai 18	Chai et al. (2022)
	QPh.caas-4D.1	E2/E3/E4/E5/E6/E7/E8/E9/E10/E11/E12/E13/E14	58.0–58.1	*AX-89703298*	*AX-110572006*	46.09	40.10	11.19	Zhoumai 18	Peng et al. (1999)
	QPh.caas-5D.1	E5/E7/E9/E10/E14	131.6–133.0	*AX-111175690*	*AX-110958036*	6.58	2.41	-2.74	Hengguan 35	NA
	QPh.caas-5D.2	E2/E3/E6/E13	173.9–174.0	*AX-109534644*	*AX-110295931*	6.54	2.81	-2.62	Hengguan 35	Zhao et al. (2018)
GN	*QGn.caas-2A.2*	E3/E7/E10/E11/E14	59.7–60.3	*AX-111466604*	*AX-110620573*	4.64	3.29	1.21	Hengguan 35	NA
	QGn.caas-4A.4	E3/E7/E13	162.7–163.0	*AX-95220664*	*AX-94503747*	8.23	5.18	1.98	Hengguan 35	Gao et al. (2015)
	QGn.caas-5A.4	E7/E8/E14	82.1–82.8	*AX-109343369*	*AX-108832618*	5.37	2.88	1.09	Hengguan 35	NA
	QGn.caas-7A.2	E3/E4/E8/E12/E13/E14	170.9–173.6	*AX-109279553*	*AX-110721033*	6.14	4.76	-1.63	Zhoumai 18	Kuzay et al. (2022)
	QGn.caas-3B.1	E5/E6/E9/E14	1.0–1.2	*AX-110468825*	*AX-111556751*	6.45	4.13	1.57	Hengguan 35	NA
	QGn.caas-5B.1	E3/E9/E11	13.1–14.9	*AX-110416577*	*AX-109866963*	7.23	4.39	1.67	Hengguan 35	NA
	QGn.caas-4D.1	E2/E3/E4/E5/E6/E7/E8/E9/E10/E11/E12/E13/E14	56.7–62.7	*AX-108944764*	*AX-111354775*	25.29	21.90	-3.59	Zhoumai 18	Jia et al. (2013)
TGW	*QTgw.caas-3A.2*	E5/E11/E14	218.5–219.0	*AX-111079045*	*AX-109872128*	7.51	4.28	-1.31	Zhoumai 18	NA
	QTgw.caas-4A.5	E2/E5/E9/E13/E14	142.0–143.0	*AX-109857541*	*AX-108966947*	7.81	6.03	-1.32	Zhoumai 18	Gao et al. (2015)
	QTgw.caas-4A.6	E1/E3/E6/E7/E8	162.9–171.2	*AX-95220664*	*AX-111600193*	8.00	7.09	-1.49	Zhoumai 18	Guan et al. (2018)

Table 2 (continued)

Trait[a]	QTL	Environment[b]	Marker interval (cM)	Left marker of peak	Right marker of peak	LOD[c]	PVE (%)[d]	Add[e]	Donor of favorable alleles	Previous reference reports[f]
	QTgw.caas-7A.1	E3/E7/E14	51.9–55.5	*AX-111761655*	*AX-109959178*	8.14	4.98	-1.24	Zhoumai 18	NA
	QTgw.caas-7A.3	E5/E9/E11/E14	165.7–170.4	*AX-111583862*	*AX-108784724*	7.66	4.78	1.37	Hengguan 35	Keeble-Gagnère et al. (2018)
	QTgw.caas-7A.6	E7/E8/E12	221.6–222.3	*AX-110554268*	*AX-109934866*	4.77	4.51	1.20	Hengguan 35	Kumar et al. (2016)
	QTgw.caas-4D.1	E1/E2/E3/E5/E6/E7/E8/E9/E10/E11/E12/E13/E14	57.0–57.8	*AX-108944764*	*AX-89703298*	28.00	27.65	3.00	Hengguan 35	Mohler et al. (2016)
GL	*QGl.caas-1A.1*	E1/E9/E11	7.7–7.9	*AX-111486000*	*AX-86178568*	5.85	5.06	0.06	Hengguan 35	NA
	QGl.caas-4A.1	E5/E8/E9/E13	141.9–146.9	*AX-111148488*	*AX-110543806*	6.63	5.88	-0.07	Zhoumai 18	NA
	QGl.caas-4A.4	E1/E2/E3/E4/E5/E7/E9/E10/E11/E14	242.2–242.5	*AX-109548008*	*AX-110952283*	6.60	4.47	-0.06	Zhoumai 18	NA
	QGl.caas-5A.1	E4/E5/E8/E10/E12/E14	1.0–1.9	*AX-110680739*	*AX-111128087*	10.15	5.64	0.07	Hengguan 35	Mohler et al. (2016)
	QGl.caas-5A.4	E4/E11/E12/E14	197.6–201.1	*AX-109423091*	*AX-109581017*	13.32	6.42	-0.07	Zhoumai 18	NA
	QGl.caas-6A.4	E10/E11/E12/E14	137.8–139.3	*AX-94815082*	*AX-89481603*	9.31	4.93	-0.06	Zhoumai 18	NA
	QGl.caas-7A.2	E2/E3/E5/E12/E13	97.2–101.5	*AX-110478459*	*AX-111628682*	3.85	3.56	0.05	Hengguan 35	Cui et al. (2016)
	QGl.caas-7A.4	E4/E7/E8/E9/E10/E12/E13/E14	173.6–179.5	*AX-109908479*	*AX-111601461*	8.77	5.90	0.07	Hengguan 35	Su et al. (2016)
	QGl.caas-3B.1	E8/E10/E11/E12	137.2–140.2	*AX-108894034*	*AX-110081374*	5.11	3.37	-0.05	Zhoumai 18	NA
	QGl.caas-4D.1	E3/E7/E9/E11	55.2–57.9	*AX-89654830*	*AX-110572006*	5.54	4.67	0.06	Hengguan 35	Peng et al. (1999)
	QGl.caas-4D.2	E2/E8/E10/E13/E14	71.9–75.8	*AX-110696146*	*AX-108726608*	12.25	7.27	0.07	Hengguan 35	NA
	QGl.caas-5D.3	E3/E4/E8/E12	135.1–139.8	*AX-110958036*	*AX-109809706*	6.52	4.60	-0.06	Zhoumai 18	Li et al. (2019)
	QGl.caas-6D.1	E2/E3/E5/E8/E9/E10/E13	0.0–3.3	*AX-94797722*	*AX-109871624*	4.98	4.37	-0.06	Zhoumai 18	NA
GW	*QGw.caas-4A.1*	E5/E11/E13	119.8–121.8	*AX-111612772*	*AX-109558533*	5.05	3.00	-0.05	Zhoumai 18	NA
	QGw.caas-4A.3	E4/E8/E9/E10/E14	141.2–142.0	*AX-109844107*	*AX-110540586*	12.37	8.42	-0.05	Zhoumai 18	Guan et al. (2018)
	QGw.caas-5A.1	E8/E10/E14	123.9–124.1	*AX-109516381*	*AX-109306311*	3.87	2.96	0.03	Hengguan 35	NA
	QGw.caas-4D.1	E1/E2/E3/E4/E5/E7/E8/E9/E10/E11/E12/E13/E14	56.8–59.3	*AX-108944764*	*AX-110572006*	21.90	22.55	0.09	Hengguan 35	Peng et al. (1999)
GT	*QGt.caas-7A.4*	E3/E5/E7/E11/E14	221.5–221.9	*AX-110362833*	*AX-111046608*	4.67	4.03	0.03	Hengguan 35	NA
	QGt.caas-2B.1	E3/E9/E10	64.0–67.1	*AX-108769797*	*AX-109364692*	4.05	3.34	0.04	Hengguan 35	NA
	QGt.caas-4D.1	E1/E2/E3/E4/E5/E7/E8/E9/E10/E11/E12/E13/E14	51.3–57.9	*AX-108735064*	*AX-110572006*	21.84	22.76	0.08	Hengguan 35	Peng et al. (1999)

[a]The abbreviated names of all the phenotypic traits are shown in Table 1. [b]E1, E2, E3, E4, E5, E6, E7, E8, E9, E10, E11, E12, E13, and E14 indicate 2014-Zhengzhou, 2015-Shunyi, 2015-Xinxiang, 2016-Shunyi, 2016-Xinxiang, 2017-Shunyi, 2017-Xinxiang, 2018-Shunyi, 2018-Xinxiang, 2019-Shunyi, 2019-Xinxiang, 2020-Shunyi, 2020-Xinxiang, and BLUP, respectively. [c]LOD, likelihood of odds; [d]PVE, proportion of phenotypic variation of the corresponding QTL; [e]ADD, additive effect; [f]NA: not available

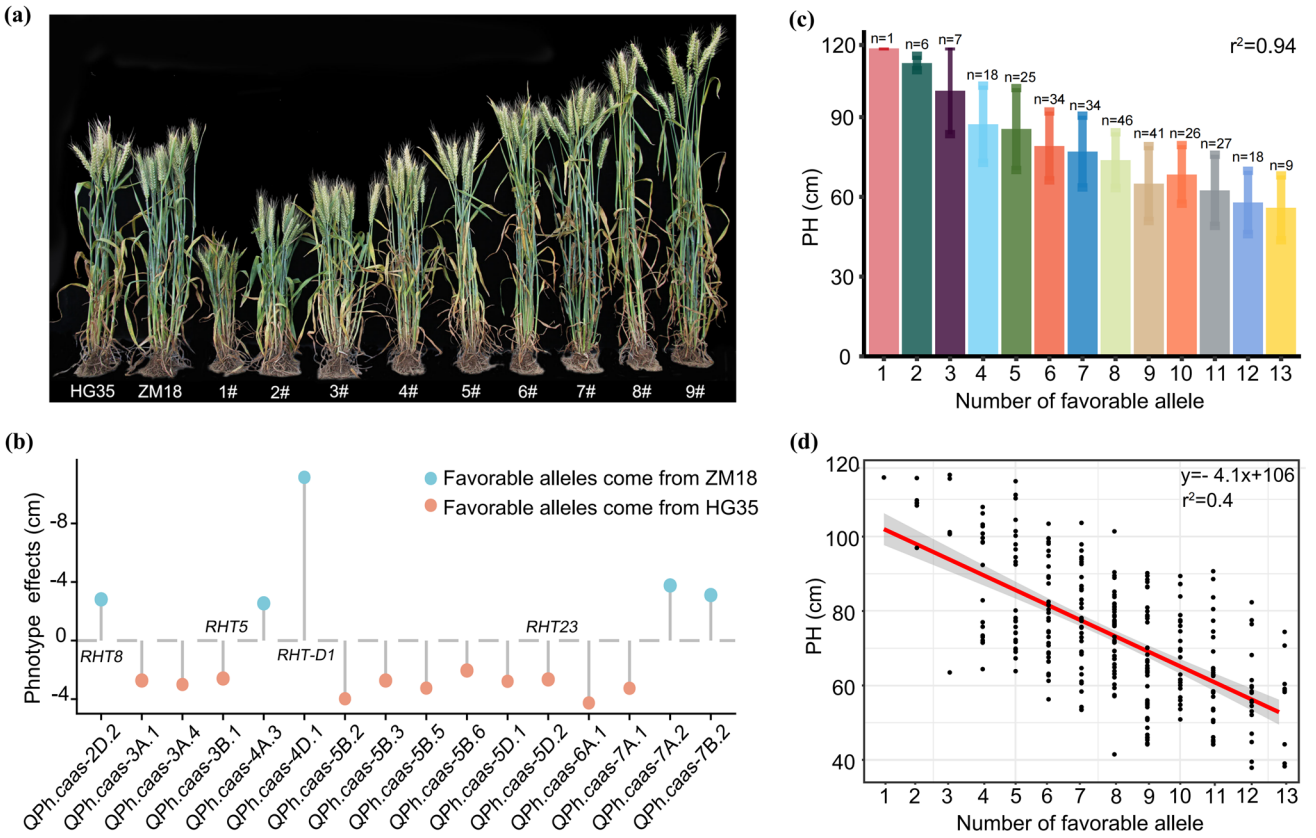

Fig. 5 Plant height variation with the accumulation of favorable alleles in the RIL population. **a** Plant height of parents and representative lines of the RIL population. HG35, Hengguan 35; ZM18, Zhoumai 18. **b** Sixteen stable QTLs associated with plant height were identified through linkage analysis in the RIL population. *RHT8*, *RHT5*, *RHT-D1*, *RHT23* represent the presence of cloned genes in the corresponding QTL region. **c** Plant heights of the accessions harboring different numbers of favorable alleles. **d** Correlations between the number of favorable alleles and plant height

Co-localized genome regions discovered by the RIL and AB-NAMIC populations

On the basis of our previous study (Jiao et al. 2023), a total of 365 QTLs controlling PH, GN, TGW, GL, GW, and GT were identified in the AB-NAMIC population via association mapping (Table S6). Thus, joint linkage analysis and association mapping in the current study revealed co-localized genomic regions for all six yield-related traits in the RIL and AB-NAMIC populations (Figs. 6 and S8). Altogether, there were 26 overlapping QTL regions for PH, GN, TGW, and GL on chromosomes 1A, 2A, 2D, 3A, 3B, 4A, 5A, 5B, 5D, 6A, and 7A between these two populations (Table S7). Among them, *QPh.caas-2D.2*, *QPh.caas-3B.1*, *QTgw.caas-4A.6*, *QTgw.caas-7A.6*, *QGl.caas-4A.1*, *QGl.caas-5A.1*, *QGl.caas-5D.3*, and *QGl.caas-7A.4* were detected in the RIL population in at least three environments, indicating an important candidate genomic region for yield-related traits to be fine-mapped in subsequent research.

Candidate genes within the GL-associated genomic region on chromosome 5A

The analysis of overlapping genome regions between the RIL and AB-NAMIC populations revealed a QTL that was simultaneously detected through both linkage analysis and GWAS, namely *QGl.caas-5A.1*, located on chromosome 5A and delimited by the flanking markers *AX-110680739* and *AX-111128087*, with a LOD value > 10 (Fig. 7a). Further analysis indicated that the physical interval of *QGl.caas-5A.1* was between 1.68 Mb and 2.73 Mb, which contained 11 high-confidence genes. The gene expression data from the Wheat Expression Browser database revealed that only three of these genes were expressed in the spike or grain, namely *TreasCS5A03G0002000*, *TreasCS5A03G0002100*, and *TreasCS5A03G0002500* (Fig. 7b). The functional annotation of *TraesCS5A03G0002500* was carotenoid cleavage dioxygenase, which was preliminarily considered the candidate gene for *QGl.caas-5A.1* (Table S8). *TraesCS5A03G0002500* has 14 exons and 13 introns, and the 660 K genotyping

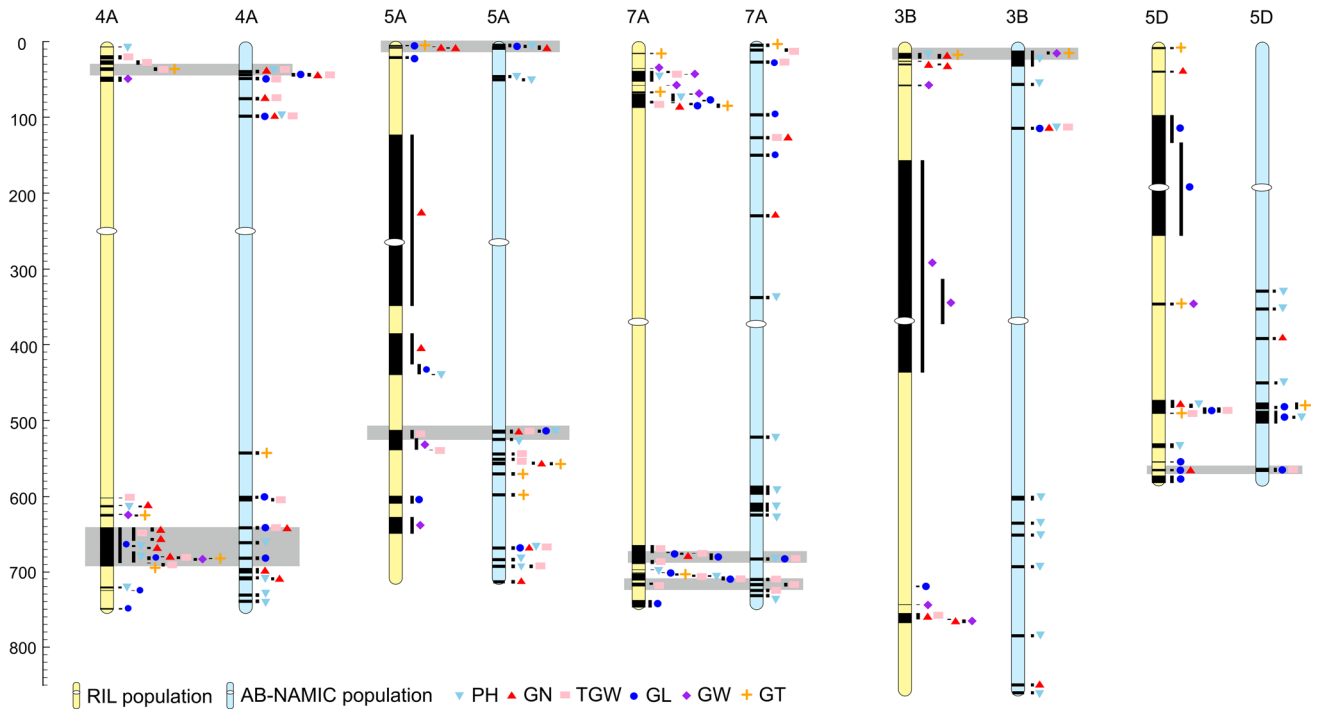

Fig. 6 QTL overlapping regions on chromosomes of the RIL and AB-NAMIC populations. Chromosomes of different colors represent the RIL population (left) and the AB-NAMIC population (right), and different shapes represent different traits. PH, GN, TGW, GL, GW, and GT represent plant height, grain number per spike, thousand-grain weight, grain length, grain width, and grain thickness, respectively. The bottom shading on the chromosomes in both populations indicates segments co-anchored by GWAS and linkage analysis. The black box beside the chromosome represents the QTL segment size

results in the RIL population revealed four SNP variations in the intron region (Fig. 7c). KASP primers were designed based on the [A/G] variation in the second intron region in *TraesCS5A03G0002500* (Table S2). Subsequently, a natural population consisting of 350 accessions was screened using the KASP marker, and the results showed that effective genotyping of both allelic and heterozygous variants (Fig. 7d, Table S1). Furthermore, a two-tailed *t*-test was conducted on four grain-related traits in the natural population carrying two types of alleles (Fig. 7e). Compared with the accessions carrying the A allele, the accessions carrying the G allele presented greater TGW, GL, GW, and GT; therefore, the G allele was the favorable allele of *TraesCS5A03G0002500* for yield-related traits.

Discussion

The rich diversity of phenotypic variations lays the foundation for QTL mapping

The phenomenon of transgressive segregation has been widely applied in agricultural production to increase crop yield and improve disease resistance and stress tolerance (Gu et al. 2023). In this study, the basic descriptive statistics of the six traits indicated that there was no significant phenotypic difference between the two parents, Hengguan 35 and Zhoumai 18, in terms of PH, TGW, and other traits, but the RILs showed extremely high phenotypic variation, especially in PH (Table 1). Cui et al. (2011) reported that there was no significant difference in PH between parents, and their offspring showed transgressive segregation, which was consistent with the results of the present study. Taking PH as an example, among the 16 identified QTLs associated with PH, 11 QTLs for reduced PH were derived from Hengguan 35, each exhibiting a relatively small additive effect within the absolute range of 2.0–4.2 cm. Meanwhile, the other five identified QTLs responsible for reducing PH were traced back to Zhoumai 18, with *QPh.caas-4D.1* exhibiting a high additive effect of 11.2 cm (Fig. 5). These results suggest that Hengguan 35 carries multiple minor-effect QTLs for reducing PH, whereas Zhoumai 18 carries a major-effect QTL for reducing PH, thus resulting in no significant difference in plant height between the parents. Furthermore, the RIL population carried varying numbers of QTLs for reduced PH, and with an increase in the number of favorable alleles, there was an obvious decrease in PH, which was consistent with the findings of Pang et al. (2020). The significant differences in PH among the offspring can be attributed to the recombination of chromosomes for

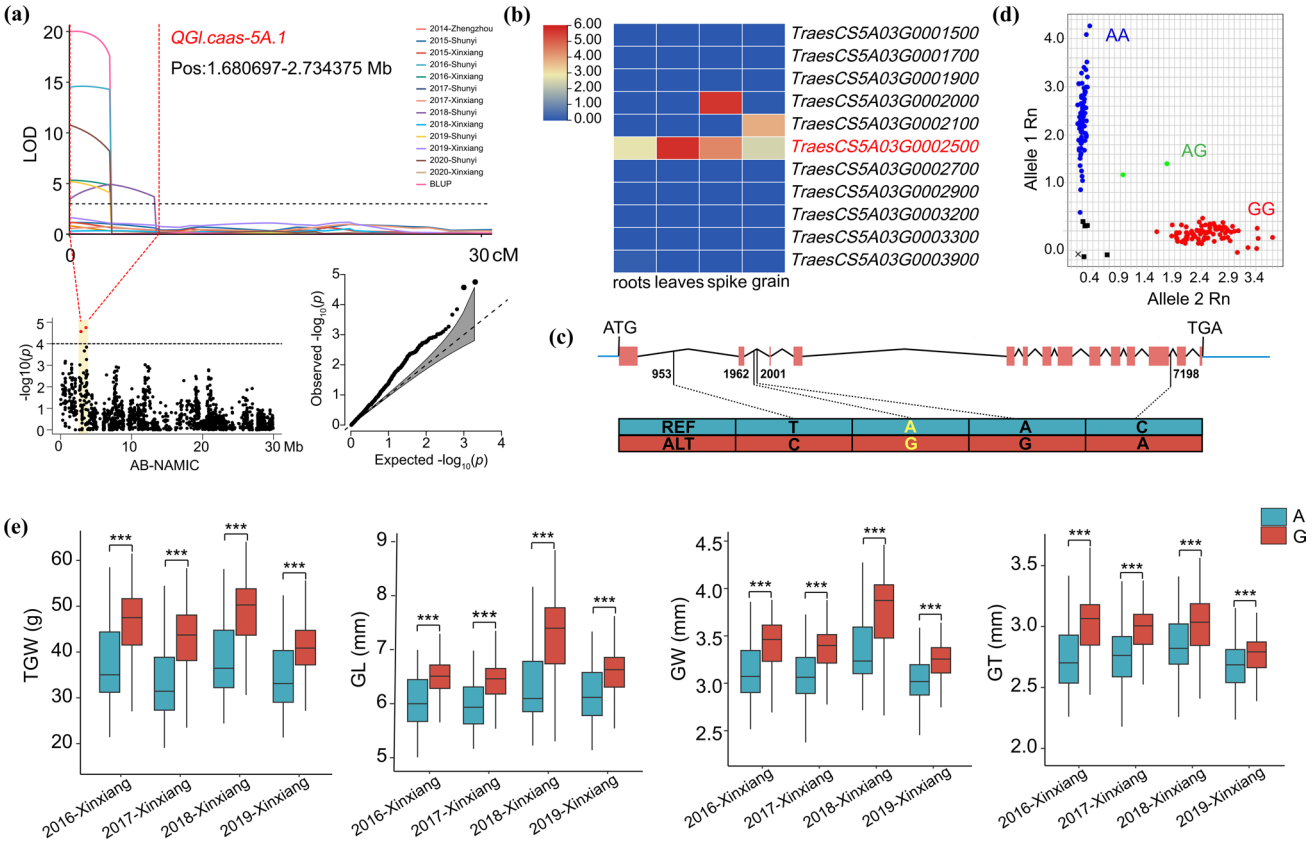

Fig. 7 Candidate gene prediction and preliminary functional validation of *QGl.caas-5A.1*. **a** *QGl.caas-5A.1* detected in the RIL and AB-NAMIC populations. **b** Transcriptome data for four tissues from Chinese Spring in the physical interval of *QGl.caas-5A.1*. **c** Structure of *TraesCS5A03G0002500*. **d** Allelic segregation of the KASP marker for *TraesCS5A03G0002500* alleles. **e** Phenotypic differences between the two alleles of *TraesCS5A03G0002500* in thousand-grain weight (TGW), grain length (GL), grain width (GW), and grain thickness (GT) across four environments

the QTLs with reducing PH during the hybridization and multi-generation self-cross of the RIL population. Simply speaking, the rich phenotypic variation in the RIL population lays the foundation for gene discovery.

QTL comparison with previous studies

The PH of wheat is a composite trait, comprising spike length and internode length below the spike. The "Green Revolution" in the 1960s introduced semidwarf genes that reduce PH, increase lodging resistance, and significantly improve grain yield (Gale and Youssefian 1985). Currently, 25 *Rht* genes have been identified on chromosomes 2A, 2B, 2D, 3B, 4A, 4B, 4D, 5A, 5D, 6A, 7A, and 7B (Mo et al. 2018). In this study, 16 stable QTLs controlling PH were identified in the RIL population. BLAST analysis revealed that *QPh.caas-2D.2*, *QPh.caas-4D.1*, *QPh.caas-5D.2*, and *QPh.caas-3B.1* contain the known genes *RHT8*, *RHT-D1*, *RHT23*, and *RHT5*, respectively (Chai et al. 2022; Peng et al. 1999; Zhao et al. 2018; Cui et al. 2022). *QPh.caas-4D.1* simultaneously affects TGW, GL, GW, GT, as well as GN. Furthermore, *QPh.caas-3A.1*, *QPh.caas-3A.4*, *QPh.caas-4A.3*, *QPh.caas-6A.1*, *QPh.caas-7A.2*, and *QPh.caas-7B.2* overlapped with the loci for PH reported in previous studies (Zhang et al. 2017; Guan et al. 2018; Li et al. 2015; Zhai et al. 2016; Hu et al. 2020; Yan et al. 2006). However, six new loci controlling PH were identified in the current study, four of which were located on chromosome 5B. Generally, the GN depends on the fertility of the florets and the number of spikelet per spike, which is determined in the early stages of spikelet development (Xiao et al. 2022). In the present study, *QGn.caas-7A.2* contained the cloned *WAPO1* gene (Kuzay et al. 2022). *QGn.caas-4D.1* and *QGn.caas-4A.4* identified through linkage analysis were consistent with those reported by Jia et al. (2013) and Gao et al. (2015). Other stable QTLs, which represent new loci controlling spikelet numbers and grain numbers, have not been previously reported. Increasing yield is significantly correlated with an increase in TGW, with seed size being a crucial factor in determining grain weight. In this study, seven stable QTLs related to grain weight were identified in the RIL population, of which *QTgw.caas-4A.5*, *QTgw.*

caas-4A.6, *QTgw.caas-7A.3*, *QTgw.caas-7A.6*, and *QTgw.caas-4D.1* were consistent with previous studies (Gao et al. 2015; Guan et al. 2018; Keeble-Gagnère et al. 2018; Kumar et al 2016; Mohler et al. 2016), which indicates that these QTLs are stable in different genetic backgrounds. Additionally, only two TGW-related QTLs were most likely novel loci. Starch synthesis plays a significant role in regulating seed size, with starch synthesis-related genes *TaSus1* and *Tasus2* being associated with seed size (Jiang et al. 2011; Hou et al. 2014). However, the genetic loci underlying wheat seed size are poorly understood. This study identified several QTLs associated with GL, GW, and GT, some of which overlapped with previously reported QTLs (Mohler et al. 2016; Cui et al. 2016; Su et al. 2016; Li et al. 2019; Guan et al. 2018). Additionally, several QTLs located on chromosomes 1A, 4A, 5A, 6A, 7A, 2B, 3B, 4D, and 6D are novel loci associated with grain size. Taken together, these data are largely consistent with previous findings and provide novel targets for the discovery of genes underlying yield-related traits in wheat.

QTL clusters for yield-related traits

Pleiotropy is a critical factor influencing the mutation and evolution of biological traits. This phenomenon plays a key role in the inheritance, evolution, and development of crops, making it especially valuable for strategies such as pyramiding breeding and MAS (Deng et al. 2017). QTL cluster analysis provides essential insights into deciphering the genetic regulatory networks of complex traits and the mechanisms underlying trait-trait correlations. Previous studies identified several QTL clusters associated with PH, TGW, GL, and GW (Ren et al. 2021), and a major QTL cluster spanning chromosome 3AS (between *wsnp_Ku_c50833_56310208* and *wsnp_Ra_c19079_28210937*) governing spike length, grain number per spike, spikelet numbers per spike, and total spikelet number per spike (Liu et al. 2018a, b). This study demonstrated that multiple QTL clusters regulated PH, GN, and grain weight-related traits (TGW, GL, GW, GT) through synergistic or antagonistic effects, revealing the genetic relatedness among these traits. Among the ten pleiotropic QTL clusters identified in this study, the *QGt.caas-4D.1/QGl.caas-4D.1/QGn.caas-4D.1/QGw.caas-4D.1/QTgw.caas-4D.1/QPh.caas-4D.1* cluster negatively regulates PH/GN and positively regulates PH/TGW, explaining the significant negative correlation between PH and GN, as well as the positive correlation between PH and TGW (Fig. 2, Table S5). The additive effect directions of QTL clusters further help optimize breeding strategy. For instance, the antagonistic additive effects of *QTgw.caas-7A.3* (+ 1.37 g) and *QGn.caas-7A.2* (-1.63) in the Q*Tgw.caas-7A.3/QGn.caas-7A.2/QGl.caas-7A.4* cluster directly validate the TGW/GN trade-off, highlighting the importance of designing allele pyramiding strategies targeting specific QTL clusters in MAS. In summary, the study and application of pleiotropic QTLs offer novel insights and approaches for crop genetic improvement, particularly in the selection and optimization of complex traits.

Joint linkage analysis and association mapping provide a new perspective for discovering yield-related genes

Currently, research focused on the genetic basis dissection of crop quantitative traits by using artificial genetic populations is increasing. Generally, the construction of parental populations is relatively simple and has high QTL detection efficacy. The advanced backcross-nested association mapping (AB-NAM) population combines the characteristics of the advanced backcross (AB) and nested association mapping (NAM) populations and has become an effective population for mining new loci of exotic germplasm resources (Nice et al. 2016). In the previous study, an AB-NAMIC population was developed by crossing three elite Chinese wheat cultivars with approximately 20 accessions from a mini core collection of Chinese wheat genetic resources, and in this population, rare alleles were strongly detected (Jiao et al. 2023). Given these findings for the AB-NAMIC population, a combination of the mapping results of the RIL and AB-NAMIC populations was attempted to explore QTLs that can be consistently identified across different genetic backgrounds. By joint linkage analysis and association mapping, 26 overlapping genomic regions were identified (Table S7, Fig. 6), which should be the focus of further research. However, the yield-related traits of wheat are controlled by multiple genes and are susceptible to environmental influences, and the distance of genomic linkage disequilibrium ($\geq$ 2 Mb) of wheat is much greater than that of rice, maize, and other crops (Li et al. 2022; Jiao et al. 2023). Thus, it is still challenging to identify genetic loci related to yield traits in candidate regions. Therefore, for QTLs with large genomic intervals identified across both panels, such as *QGl.caas-4A.2*, located in the 641.8–688.5 Mb region on chromosome 4A, it is essential to employ a combination of methodologies such as bulked segregant analysis (BSA), bulk segregant RNA sequencing (BSR-seq), and RNA sequencing (RNA-seq) for further fine mapping of potential candidate genes (Zhao et al. 2023).

In the current study, one stable QTL, *QGl.caas-5A.1*, was associated with GL, and contained relatively small candidate regions for further exploration of the candidate gene (Fig. 7). Candidate genes were predicted based on gene expression data in different tissues and functional annotations of the homologous gene. Those results lay a solid foundation for

the subsequent cloning of yield-related genes. In the future, functional validation of target genes will be conducted via overexpression and clustered regularly interspaced palindromic repeats (CRISPR)/Cas9 technologies, aiming to elucidate the molecular mechanisms underlying GL and other yield-related traits.

Conclusions

In this study, a high-quality genetic map spanning 4,243.31 cM was constructed using data from the Affymetrix wheat 660 K SNP array. An RIL population was used to identify QTLs for yield-related traits, *i.e.*, PH, GN, TGW, GL, GW, and GT in multiple environments. A total of 50 stable QTLs were identified in more than three environments. The pyramiding of favorable alleles detected in this study indicated highly positive phenotypic effects on all the traits. Joint linkage analysis and association mapping discovered 26 overlapping QTLs. Notably, *TraesCS5A03G0002500* was selected as the candidate gene of *QGl.caas-5A.1* for grain length. Furthermore, a KASP marker was developed based on the [A/G] variation of *TraesCS5A03G0002500* and verified in a natural population. The G allele was found to be favorable and was associated with higher TGW, GL, GW, and GT. These findings provide new insights into dissecting the genetic basis of yield-related traits and molecular-assisted breeding and lay the foundation for cloning and molecular mechanism analysis of yield-related genes.

Supplementary Information The online version contains supplementary material available at https://doi.org/10.1007/s00122-025-04900-4.

Author contribution statement CH designed the experiments and edited the manuscript; LZ performed the experiments and wrote the manuscript; LD constructed the RIL population; HL participated in the experiments and data analyses; HL, HL, YZ, YL, JH, and TL participated in phenotypic investigation; DY participated in data analyses and revising the manuscript; XZ participated in field trials and revising the manuscript. All authors contributed to the article and approved the final manuscript.

Funding This work was financially supported by grants from the STI 2030-Major Projects (2023ZD0406802), the Biological Breeding-National Science and Technology Major Project (2022ZD04017), the National Key Research and Development Program of China (2023YFD1200404), and the Innovation Program of Chinese Academy of Agricultural Sciences (CAAS-CSCB-202401).

Data availability Data generated in this study are available from the corresponding author upon reasonable request.

Declarations

Competing interests The authors declare that there is no conflict of interest.

References

Al-Sheikh Ahmed S, Zhang JJ, Ma WJ, Dell B (2018) Contributions of *TaSUTs* to grain weight in wheat under drought. Plant Mol Biol 98:333–347. https://doi.org/10.1007/s11103-018-0782-1

Bates D, Mächler M, Bolker B, Walker S (2015) Fitting linear mixed-effects models using lme4. J Stat Softw 67(1):1–48. https://doi.org/10.18637/jss.v067.i01

Bergelson J, Roux F (2010) Towards identifying genes underlying ecologically relevant traits in *Arabidopsis thaliana*. Nat Rev Genet 11(12):867–879. https://doi.org/10.1038/nrg2896

Cadic E, Coque M, Vear F, Grezes-Besset B, Pauquet J, Piquemal J, Lippi Y, Blanchard P, Romestant M, Pouilly N, Rengel D, Gouzy J, Langlade N, Mangin B, Vincourt P (2013) Combined linkage and association mapping of flowering time in Sunflower (*Helianthus annuus* L.). Theor Appl Genet 126(5):1337–1356. https://doi.org/10.1007/s00122-013-2056-2

Cao J, Liu KY, Song WJ, Zhang JN, Yao YY, Xin MM, Hu ZR, Peng HR, Ni ZF, Sun QX (2021) Pleiotropic function of the squamosa promoter-binding protein-like gene *TaSPL14* in wheat plant architecture. Planta 253(2):44. https://doi.org/10.1007/s00425-020-03531-x

Chai LL, Xin MM, Dong CQ, Chen ZY, Zhai HJ, Zhuang JH, Cheng XJ, Wang NJ, Geng J, Wang XB, Bian RL, Yao YY, Guo WL, Hu ZR, Peng HR, Bai GH, Sun QX, Su ZQ, Liu J, Ni ZF (2022) A natural variation in Ribonuclease H-like gene underlies *Rht8* to confer "Green Revolution" trait in wheat. Mol Plant 15(3):377–380. https://doi.org/10.1016/j.molp.2022.01.013

Cheng XJ, Xin MM, Xu RB, Chen ZY, Cai WL, Chai LL, Xu HW, Jia L, Feng ZY, Wang ZH, Peng HR, Yao YY, Hu ZR, Guo WL, Ni ZF, Sun QX (2020) A single amino acid substitution in STKc_GSK3 kinase conferring semispherical grains and its implications for the origin of *Triticum sphaerococcum*. Plant Cell 32(4):923–934. https://doi.org/10.1105/tpc.19.00580

Cui F, Fan XL, Chen M, Zhang N, Zhao CH, Zhang W, Han J, Ji J, Zhao XQ, Yang LJ, Zhao ZW, Tong YP, Wang T, Li JM (2016) QTL detection for wheat kernel size and quality and the responses of these traits to low nitrogen stress. Theor Appl Genet 129(3):469–484. https://doi.org/10.1007/s00122-015-2641-7

Cui F, Zhang N, Fan XL, Zhang W, Zhao CH, Yang LJ, Pan RQ, Chen M, Han J, Zhao XQ, Ji J, Tong YP, Zhang HX, Jia JZ, Zhao GY, Li JM (2017) Utilization of a Wheat660K SNP array-derived high-density genetic map for high-resolution mapping of a major QTL for kernel number. Sci Rep 7(1):3788. https://doi.org/10.1038/s41598-017-04028-6

Cui C, Lu QM, Zhao ZC, Lu S, Duan S, Yang Y, Qiao Y, Chen L, Hu YG (2022) The fine mapping of dwarf gene *Rht5* in bread wheat

and its effects on plant height and main agronomic traits. Planta 255(6):114. https://doi.org/10.1007/s00425-022-03888-1

Cui F, Li J, Ding AM, Zhao CH, Wang L, Wang XQ, Li SS, Bao YG, Li XF, Feng DS, Kong LR, Wang HG (2011) Conditional QTL mapping for plant height with respect to the length of the spike and internode in two mapping populations of wheat. Theor Appl Genet 122(8):1517–1536. https://doi.org/10.1007/s00122-011-1551-6

Danecek P, Auton A, Abecasis G, Albers CA, Banks E, DePristo MA, Handsaker RE, Lunter G, Marth GT, Sherry ST, McVean G, Durbin R; 1000 Genomes Project Analysis Group (2011) The variant call format and VCFtools. Bioinformatics 27(15):2156–2158. https://doi.org/10.1093/bioinformatics/btr330

Deng Z, Cui Y, Han Q, Fang W, Li J, Tian J (2017) Discovery of consistent QTLs of wheat spike-related traits under nitrogen treatment at different development stages. Front Plant Sci 8:2120

Finnegan EJ, Ford B, Wallace X, Pettolino F, Griffin PT, Schmitz RJ, Zhang P, Barrero JM, Hayden MJ, Boden SA, Cavanagh CA, Swain SM, Trevaskis B (2018) Zebularine treatment is associated with deletion of *FT-B1* leading to an increase in spikelet number in bread wheat. Plant Cell Environ 41(6):1346–1360. https://doi.org/10.1111/pce.13164

Gale MD, Youssefian S (1985) Dwarfing genes in wheat. Progress in Plant Breeding-1. Butterworth: Elsevier Inc. p. 1–35

Gao FM, Wen WE, Liu JD, Rasheed A, Yin GH, Xia XC, Wu XX, He ZH (2015) Genome-wide linkage mapping of QTL for yield components, plant height and yield-related physiological traits in the Chinese wheat cross Zhou 8425B/Chinese Spring. Front Plant Sci 6:1099. https://doi.org/10.3389/fpls.2015.01099

Gu ZG, Gu L, Eils R, Schlesner M, Brors B (2014) circlize Implements and enhances circular visualization in R. Bioinformatics 30(19):2811–2812. https://doi.org/10.1093/bioinformatics/btu393

Gu ZL, Gong JY, Zhu Z, Li Z, Feng Q, Wang CS, Zhao Y, Zhan QL, Zhou CC, Wang AH, Huang T, Zhang L, Tian QL, Fan DL, Lu YQ, Zhao Q, Huang XH, Yang SH, Han B (2023) Structure and function of rice hybrid genomes reveal genetic basis and optimal performance of heterosis. Nat Genet 55(10):1745–1756. https://doi.org/10.1038/s41588-023-01495-8

Guan PF, Lu LH, Jia LJ, Kabir MR, Zhang JB, Lan TY, Zhao Y, Xin MM, Hu ZR, Yao YY, Ni ZF, Sun QX, Peng HR (2018) Global QTL analysis identifies genomic regions on chromosomes 4A and 4B harboring stable loci for yield-related traits across different environments in wheat (*Triticum aestivum* L.). Front Plant Sci 25(9):529. https://doi.org/10.3389/fpls.2018.00529

Gupta PK, Balyan HS, Sharma S, Kumar R (2020) Genetics of yield, abiotic stress tolerance and biofortification in wheat (*Triticum aestivum* L.). Theor Appl Genet 133(5):1569–1602. https://doi.org/10.1007/s00122-020-03583-3

Hong YT, Chen LF, Du LP, Su ZQ, Wang JF, Ye XG, Qi L, Zhang ZY (2014) Transcript suppression of *TaGW2* increased grain width and weight in bread wheat. Funct Integr Genom 14(2):341–349. https://doi.org/10.1007/s10142-014-0380-5

Hou J, Jiang QY, Hao CY, Wang YQ, Zhang HN, Zhang XY (2014) Global selection on sucrose synthase haplotypes during a century of wheat breeding. Plant Physiol 164(4):1918–1929. https://doi.org/10.1104/pp.113.232454

Hu JM, Wang XQ, Zhang GX, Jiang P, Chen WY, Hao YC, Ma X, Xu SS, Jia JZ, Kong LR, Wang HM (2020) QTL mapping for yield-related traits in wheat based on four RIL populations. Theor Appl Genet 133(3):917–933. https://doi.org/10.1007/s00122-019-03515-w

Huang XZ, Qian Q, Liu ZB, Sun HY, He SY, Luo D, Xia GM, Chu CC, Li JY, Fu XD (2009) Natural variation at the *DEP1* locus enhances grain yield in rice. Nat Genet 41(4):494–497. https://doi.org/10.1038/ng.352

Huang K, Wang DK, Duan PG, Zhang BL, Xu R, Li N, Li YH (2017) *WIDE AND THICK GRAIN 1*, which encodes an otubain-like protease with deubiquitination activity, influences grain size and shape in rice. Plant J 91(5):849–860. https://doi.org/10.1111/tpj.13613

Jia HY, Wan HS, Yang SH, Zhang ZZ, Kong ZX, Xue SL, Zhang LX, Ma ZQ (2013) Genetic dissection of yield-related traits in a recombinant inbred line population created using a key breeding parent in China's wheat breeding. Theor Appl Genet 126(8):2123–2139. https://doi.org/10.1007/s00122-013-2123-8

Jiang QY, Hou J, Hao CY, Wang LF, Ge HM, Dong YS, Zhang XY (2011) The wheat (T. *aestivum*) sucrose synthase 2 gene (*TaSus2*) active in endosperm development is associated with yield traits. Funct Integr Genom 11(1):49–61. https://doi.org/10.1007/s10142-010-0188-x

Jiao CZ, Hao CY, Li T, Bohra A, Wang LF, Hou J, Liu HX, Liu H, Zhao J, Wang YM, Liu YC, Wang ZW, Jing X, Wang XE, Varshney RK, Fu JJ, Zhang XY (2023) Fast integration and accumulation of beneficial breeding alleles through an AB-NAMIC strategy in wheat. Plant Commun 4(3):100549. https://doi.org/10.1016/j.xplc.2023.100549

Keeble-Gagnère G, Rigault P, Tibbits J, Pasam R, Hayden M, Forrest K, Frenkel Z, Korol A, Huang BE, Cavanagh C, Taylor J, Abrouk M, Sharpe A, Konkin D, Sourdille P, Darrier B, Choulet F, Bernard A, Rochfort S, Dimech A, Watson-Haigh N, Baumann U, Eckermann P, Fleury D, Juhasz A, Boisvert S, Nolin MA, Doležel J, Šimková H, Toegelová H, Šafář J, Luo MC, Câmara F, Pfeifer M, Isdale D, Nyström-Persson J, Iwgsc KDH, Tinning M, Cui DQ, Ru ZG, Appels R (2018) Optical and physical mapping with local finishing enables megabase-scale resolution of agronomically important regions in the wheat genome. Genome Biol 19(1):112. https://doi.org/10.1186/s13059-018-1475-4

Khan SU, Saeed S, Khan MHU, Fan C, Ahmar S, Arriagada O, Shahzad R, Branca F, Mora-Poblete F (2021) Advances and challenges for QTL analysis and GWAS in the plant-breeding of high-yielding: a focus on rapeseed. Biomolecules 11(10):1516. https://doi.org/10.3390/biom11101516

Kumar A, Mantovani EE, Seetan R, Soltani A, Echeverry-Solarte M, Jain S, Simsek S, Doehlert D, Alamri MS, Elias EM, Kianian SF, Mergoum M (2016) Dissection of genetic factors underlying wheat kernel shape and size in an Elite×Nonadapted cross using a high density SNP linkage map. Plant Genome. https://doi.org/10.3835/plantgenome2015.09.0081

Kuzay S, Lin HQ, Li CX, Chen SS, Woods DP, Zhang JL, Lan TY, Von Korff M, Dubcovsky J (2022) *WAPO-A1* is the causal gene of the 7AL QTL for spikelet number per spike in wheat. PLoS Genet 18(1):e1009747. https://doi.org/10.1371/journal.pgen.1009747

Li LH, Li XQ (2006) Descriptors and Data Standard for wheat. China Agriculture Press, Beijing

Li HH, Ribaut JM, Li ZL, Wang JK (2008) Inclusive composite interval mapping (ICIM) for digenic epistasis of quantitative traits in biparental populations. Theor Appl Genet 116:243–260. https://doi.org/10.1007/s00122-007-0663-5

Li YB, Fan CC, Xing YZ, Jiang YH, Luo LJ, Sun L, Shao D, Xu CJ, Li XH, Xiao JH, He YQ, Zhang QF (2011) Natural variation in *GS5* plays an important role in regulating grain size and yield in rice. Nat Genet 43(12):1266–1269. https://doi.org/10.1038/ng.977

Li C, Bai GH, Carver BF, Chao S, Wang Z (2015) Mapping quantitative trait loci for plant adaptation and morphology traits in wheat using single nucleotide polymorphisms. Euphytica 208(2):299–312. https://doi.org/10.1007/s10681-015-1594-x

Li FJ, Wen WE, Liu JD, Zhang Y, Cao SH, He ZH, Rasheed A, Jin H, Zhang C, Yan J, Zhang PZ, Wan YX, Xia XC (2019) Genetic architecture of grain yield in bread wheat based on genome-wide association studies. BMC Plant Biol 19(1):168. https://doi.org/10.1186/s12870-019-1781-3

Li AL, Hao CY, Wang ZY, Geng SF, Jia ML, Wang F, Han X, Kong XC, Yin LJ, Tao S, Deng ZY, Liao RY, Sun GL, Wang K, Ye

XG, Jiao CZ, Lu HF, Zhou Y, Liu DC, Fu XD, Zhang XY, Mao L (2022) Wheat breeding history reveals synergistic selection of pleiotropic genomic sites for plant architecture and grain yield. Mol Plant 15(3):504–519. https://doi.org/10.1016/j.molp.2022.01.004

Liang Y, Liu HJ, Yan J, Tian F (2021) Natural variation in crops: realized understanding, continuing promise. Annu Rev Plant Biol 72:357–385. https://doi.org/10.1146/annurev-arplant-080720-090632

Liu JJ, Luo W, Qin NN, Ding PY, Zhang H, Yang CC, Mu Y, Tang HP, Liu YX, Li W, Jiang QT, Chen GY, Wei YM, Zheng YL, Liu CJ, Lan XJ, Ma J (2018a) A 55 K SNP array-based genetic map and its utilization in QTL mapping for productive tiller number in common wheat. Theor Appl Genet 131(11):2439–2450. https://doi.org/10.1007/s00122-018-3164-9

Liu K, Sun XX, Ning TY, Duan XX, Wang QL, Liu TT, An YL, Guan X, Tian JC, Chen JS (2018b) Genetic dissection of wheat panicle traits using linkage analysis and a genome-wide association study. Theor Appl Genet 131(5):1073–1090. https://doi.org/10.1007/s00122-018-3059-9

Lopes MS, Reynolds MP, Manes Y, Singh RP, Crossa J, Braun HJ (2012) Genetic yield gains and changes in associated traits of CIMMYT spring bread wheat in a "Historic" set representing 30 years of breeding. Crop Sci 52(3):1123–1131. https://doi.org/10.2135/cropsci2011.09.0467

McIntosh RA, Dubcovsky J, Rogers WJ, Xia XC, Raupp WJ (2020) Catalogue of gene symbols for wheat: 2020 supplement. In: 13th Int Wheat Genet Symp

Meng L, Li HH, Zhang LY, Wang JK (2015) QTL IciMapping: Integrated software for genetic linkage map construction and quantitative trait locus mapping in biparental populations. Crop J 3(3):269–283. https://doi.org/10.1016/j.cj.2015.01.001

Mo Y, Vanzetti LS, Hale I, Spagnolo EJ, Guidobaldi F, Al-Oboudi J, Odle N, Pearce S, Helguera M, Dubcovsky J (2018) Identification and characterization of *Rht25*, a locus on chromosome arm 6AS affecting wheat plant height, heading time, and spike development. Theor Appl Genet 131(10):2021–2035. https://doi.org/10.1007/s00122-018-3130-6

Mohler V, Albrecht T, Castell A, Diethelm M, Schweizer G, Hartl L (2016) Considering causal genes in the genetic dissection of kernel traits in common wheat. J Appl Genet 57(4):467–476. https://doi.org/10.1007/s13353-016-0349-2

Niaz M, Zhang LR, Lv GG, Hu HT, Yang X, Cheng YZ, Zheng YT, Zhang BY, Yan XN, Htun A, Zhao L, Sun CW, Zhang N, Ren Y, Chen F (2023) Identification of *TaGL1-B1* gene controlling grain length through regulation of jasmonic acid in common wheat. Plant Biotechnol J 21(5):979–989. https://doi.org/10.1111/pbi.14009

Nice LM, Steffenson BJ, Brown-Guedira GL, Akhunov ED, Liu C, Kono TJY, Morrell PL, Blake TK, Horsley RD, Smith KP, Muehlbauer GJ (2016) Development and genetic characterization of an advanced backcross-nested association mapping (AB-NAM) population of wild×cultivated barley. Genetics 203(3):1453–1467. https://doi.org/10.1534/genetics.116.190736

Ott J, Wang J, Leal SM (2015) Genetic linkage analysis in the age of whole-genome sequencing. Nat Rev Genet 16(5):275–284. https://doi.org/10.1038/nrg3908

Ouellette LA, Reid RW, Blanchard SG, Brouwer CR (2017) LinkageMapView-rendering high-resolution linkage and QTL maps. Bioinformatics 34(2):306–307. https://doi.org/10.1093/bioinformatics/btx576

Pang YL, Liu CX, Wang DF, St Amand P, Bernardo A, Li WH, He F, Li LZ, Wang LM, Yuan XF, Dong L, Su Y, Zhang HR, Zhao M, Liang YL, Jia HZ, Shen XT, Lu Y, Jiang HM, Wu YY, Li AF, Wang HG, Kong LR, Bai GH, Liu SB (2020) High-resolution genome-wide association study identifies genomic regions and candidate genes for important agronomic traits in wheat. Mol Plant 13(9):1311–1327. https://doi.org/10.1016/j.molp.2020.07.008

Peng J, Richards DE, Hartley NM, Murphy GP, Devos KM, Flintham JE, Beales J, Fish LJ, Worland AJ, Pelica F, Sudhakar D, Christou P, Snape JW, Gale MD, Harberd NP (1999) "Green revolution" genes encode mutant gibberellin response modulators. Nature 400(6741):256–261. https://doi.org/10.1038/22307

Qi P, Lin YS, Song XJ, Shen JB, Huang W, Shan JX, Zhu MZ, Jiang L, Gao JP, Lin HX (2012) The novel quantitative trait locus *GL3.1* controls rice grain size and yield by regulating Cyclin-T1;3. Cell Res 22(12):1666–1680. https://doi.org/10.1038/cr.2012.151

Quintero A, Molero G, Reynolds MP, Calderini DF (2018) Trade-off between grain weight and grain number in wheat dependson G×E interaction: a case study of an elite CIMMYT panel(CIMCOG). Eur J Agron 92:17–29. https://doi.org/10.1016/j.eja.2017.09.007

Rasheed A, Hao YF, Xia XC, Khan A, Xu YB, Varshney RK, He ZH (2017) Crop breeding chips and genotyping platforms: progress, challenges, and perspectives. Mol Plant 10(8):1047–1064. https://doi.org/10.1016/j.molp.2017.06.008

Ren TH, Fan T, Chen SL, Li CS, Chen YY, Ou X, Jiang Q, Ren ZL, Tan FQ, Luo PG, Chen C, Li Z (2021) Utilization of a Wheat55K SNP array-derived high-density genetic map for high-resolution mapping of quantitative trait loci for important kernel-related traits in common wheat. Theor Appl Genet 134(3):807–821. https://doi.org/10.1007/s00122-021-03765-8

Sakuma S, Golan G, Guo ZF, Ogawa T, Tagiri A, Sugimoto K, Bernhardt N, Brassac J, Mascher M, Hensel G, Ohnishi S, Jinno H, Yamashita Y, Ayalon I, Peleg Z, Schnurbusch T, Komatsuda T (2019) Unleashing floret fertility in wheat through the mutation of a homeobox gene. Proc Natl Acad Sci USA 116(11):5182–5187. https://doi.org/10.1073/pnas.1815465116

Sazonovs A, Barrett JC (2018) Rare-variant studies to complement genome-wide association studies. Annu Rev Genom Hum Genet 19:97–112. https://doi.org/10.1146/annurev-genom-083117-021641

Simmonds J, Scott P, Leverington-Waite M, Turner AS, Brinton J, Korzun V, Snape J, Uauy C (2014) Identification and independent validation of a stable yield and thousand grain weight QTL on chromosome 6A of hexaploid wheat (*Triticum aestivum* L.). BMC Plant Biol 14:191. https://doi.org/10.1186/s12870-014-0191-9

Song XJ, Huang W, Shi M, Zhu MZ, Lin HX (2007) A QTL for rice grain width and weight encodes a previously unknown RING-type E3 ubiquitin ligase. Nat Genet 39(5):623–630. https://doi.org/10.1038/ng2014

Stam PA (1993) Construction of integrated genetic linkage maps by means of a new computer package: Join Map. Plant J 3:739–744. https://doi.org/10.1111/j.1365-313X.1993.00739.x

Su ZQ, Jin SJ, Lu Y, Zhang GR, Chao S, Bai GH (2016) Single nucleotide polymorphism tightly linked to a major QTL on chromosome 7A for both kernel length and kernel weight in wheat. Mol Breed 36:15. https://doi.org/10.1007/s11032-016-0436-4

Sun SY, Wang L, Mao HL, Shao L, Li XH, Xiao JH, Ouyang Y, Zhang QF (2018) A G-protein pathway determines grain size in rice. Nat Commun 9(1):851. https://doi.org/10.1038/s41467-018-03141-y

Sun CW, Dong ZD, Zhao L, Ren Y, Zhang N, Chen F (2020) The Wheat 660K SNP array demonstrates great potential for marker-assisted selection in polyploid wheat. Plant Biotechnol J 18(6):1354–1360. https://doi.org/10.1111/pbi.13361

Tong HN, Liu LC, Jin Y, Du L, Yin YH, Qian Q, Zhu LH, Chu CC (2012) Dwarf and low-tillering acts as a direct downstream target of a GSK3/SHAGGY-like kinase to mediate brassinosteroid responses in rice. Plant Cell 4(6):2562–2577. https://doi.org/10.1105/tpc.112.097394

Villanueva RAM, Chen ZJ (2019) ggplot2: elegant graphics for data analysis (2nd ed.). Meas Interdiscip Res Perspect 17:160–167

Voorrips RE (2002) MapChart: software for the graphical presentation of linkage maps and QTLs. J Hered 93(1):77–78. https://doi.org/10.1093/jhered/93.1.77

Wang SS, Wu K, Qian Q, Liu Q, Li Q, Pan YJ, Ye YF, Liu XY, Wang J, Zhang JQ, Li S, Wu YJ, Fu XD (2017a) Non-canonical regulation of SPL transcription factors by a human OTUB1-like deubiquitinase defines a new plant type rice associated with higher grain yield. Cell Res 27(9):1142–1156. https://doi.org/10.1038/cr.2017.98

Wang YG, Yu HP, Tian CH, Sajjad M, Gao CX, Tong YP, Wang XF, Jiao YL (2017b) Transcriptome association identifies regulators of wheat spike architecture. Plant Physiol 175:746–757. https://doi.org/10.1104/pp.17.00694

Xiao J, Liu B, Yao YY, Guo ZF, Jia HY, Kong LR, Zhang AM, Ma WJ, Ni ZF, Xu SB, Lu F, Jiao YN, Yang WY, Lin XL, Sun SL, Lu ZF, Gao LF, Zhao GY, Cao SH, Chen Q, Zhang KP, Wang MC, Wang M, Hu ZR, Guo WL, Li GQ, Ma X, Li JM, Han FP, Fu XD, Ma ZQ, Wang DW, Zhang XY, Ling HQ, Xia GM, Tong YP, Liu ZY, He ZH, Jia JZ, Chong K (2022) Wheat genomic study for genetic improvement of traits in China. Sci China Life Sci 65(9):1718–1775. https://doi.org/10.1007/s11427-022-2178-7

Yan LL, Fu D, Li C, Blechl A, Tranquilli G, Bonafede M, Sanchez A, Valarik M, Yasuda S, Dubcovsky J (2006) The wheat and barley vernalization gene *VRN3* is an orthologue of *FT*. Proc Natl Acad Sci USA 103(51):19581–19586. https://doi.org/10.1073/pnas.0607142103

Yang X, Pan YB, Singh PK, He XY, Ren Y, Zhao L, Zhang N, Cheng SH, Chen F (2019) Investigation and genome-wide association study for Fusarium crown rot resistance in Chinese common wheat. BMC Plant Biol 19(1):153. https://doi.org/10.1186/s12870-019-1758-2

Zhai HJ, Feng ZY, Li J, Liu XY, Xiao SH, Ni ZF, Sun QX (2016) QTL Analysis of spike morphological traits and plant height in winter wheat (*Triticum aestivum* L.) using a high-density SNP and SSR-based linkage map. Front Plant Sci 7(7):1617. https://doi.org/10.3389/fpls.2016.01617

Zhang N, Fan XL, Cui F, Zhao CH, Zhang W, Zhao XQ, Yang LJ, Pan RQ, Chen M, Han J, Ji J, Liu DC, Zhao ZW, Tong YP, Zhang AM, Wang T, Li JM (2017) Characterization of the temporal and spatial expression of wheat (T*riticum aestivum* L.) plant height at the QTL level and their influence on yield-related traits. Theor Appl Genet 130(6):1235–1252. https://doi.org/10.1007/s00122-017-2884-6

Zhao KJ, Xiao J, Liu Y, Chen SL, Yuan CX, Cao AZ, You FM, Yang DL, An SM, Wang HY, Wang XE (2018) *Rht23* (5Dq′) likely encodes a *Q* homeologue with pleiotropic effects on plant height and spike compactness. Theor Appl Genet 131(9):1825–1834. https://doi.org/10.1007/s00122-018-3115-5

Zhao JJ, Wang ZW, Liu HX, Zhao J, Li T, Hou J, Zhang XY, Hao CY (2019) Global status of 47 major wheat loci controlling yield, quality, adaptation and stress resistance selected over the last century. BMC Plant Biol 19(1):5. https://doi.org/10.1186/s12870-018-1612-y

Zhao L, Zheng YT, Wang Y, Wang SS, Wang TZ, Wang CG, Chen Y, Zhang KP, Zhang N, Dong ZD, Chen F (2023) A *HST1*-like gene controls tiller angle through regulating endogenous auxin in common wheat. Plant Biotechnol J 21(1):122–135. https://doi.org/10.1111/pbi.13930

Zhou SH, Zhang JP, Che YH, Liu WH, Lu YQ, Yang XM, Li XQ, Jia JZ, Liu X, Li LL (2018) Construction of *Agropyron Gaertn.* genetic linkage maps using a wheat 660K SNP array reveals a homoeologous relationship with the wheat genome. Plant Biotechnol 16(3):818–827. https://doi.org/10.1111/tpj.14440